International Journal on Applications in Information and Communication Engineering
Volume 7 : Issue 2 : May 2021 , pp 23 –30 www.aetsjournal.com ISSN (Online) : 2394 - 6237

A Pareto Method and Topology-Based Adaptive Classification Method Query-By-Multiple Information Extraction System: Preserve Hashing

Priyadharshini A, Srikanth R, Arputha Ajitha Rose, Udhayakumar T
Department of Computer Science and Engineering,
Rathinam Technical Campus,
Coimbatore, Tamilnadu,India

Abstract - Discovering, studying, and retrieving images from an image database is image retrieval. Text-based accessible and informational image retrieval are the two most used approaches for retrieving images. Additional information retrieval techniques exist. Text-based image retrieval arranges images according to standard database administration practices. In content-based image retrieval, also known as CBIR, the image is represented and indexed based on its visual characteristics, such as its color, shape, texture, and spatial arrangement. This combination of qualities produces a full set of retrieval characteristics for photographs. Evaluate the performance of the accessible picture retrieval algorithms using a range of accuracy levels for each image type of database. Recent study reveals that query-by-one (QBO), essentially refers to searching with a simple picture, is generally insufficient to produce reasonable performance since these attributes are not accurately related to the semantic meaning of the image. Multiple content-based picture retrieval systems have adopted query-by-multiple (QBM) methodologies. However, how to improve the data exchange to highlight the most critical properties of these inputs while downplaying the less significant parts could have a substantial impact on the acquired outcomes. This one-of-a-kind information retrieval system for numerous queries stresses the combination of the Pareto front technique with efficient manifold ranking. A topology management hashing strategy will be adopted to decrease the sophistication of user input and the number of user-computer interactions.

Keywords—Information Retrieval, Multiple Query Retrieval, Efficient Manifold Ranking (EMR).

I. INTRODUCTION

Within the fields of artificial intelligence and information extraction [1–3], content-based image retrieval, commonly known as CBIR, has become an important challenge over the course of the past twenty years. Numerous picture retrieval systems that are able to process multiple inquiries have been recommended as a direct result of the study that was carried out on this subject . This research was carried out on this topic. Each query image correlates directly to the same semantic segmentation notion in the vast majority of systems, despite having a different brief history, being shot from a different angle, or actually contains a physical mechanism that belongs to the same class. This is the case even though the query images all contain the same object. This is the case despite the fact that every image possesses a unique object that belongs to the same class. These modifications are not outside the bounds of what is conceivable. This update is dependent on the exploitation of many inquiries of the same item in an effort to improve the performance of retrieval via a single query. This is the fundamental idea that will be improved upon in the new version. From now on, we are going to refer to this particular approach to multiple-query retrieval as single-semantic multiple-query retrieval. This name change will take effect immediately. Combining a number of low-level approaches is a fundamental component of a diverse range of individualism retrieval systems.



Query 1 Query 2 Query 3

A single, averaged query that is constructed using a collection of features that are extracted from the query photographs. In this work, we investigate the more challenging problem of finding images that are relevant to multiple queries expressing a range of image semantics. Specifically, we focus on the problem of obtaining photos that contain faces. More specifically, we are concerned with the challenge of locating images that have been labeled with a particular geographic location. To be more explicit, the

International Journal on Applications in Information and Communication Engineering
Volume 7 : Issue 2 : May 2021 , pp 23 –30 www.aetsjournal.com ISSN (Online) : 2394 - 6237

goal of our search is to locate photographs that are associated with one of the following categories: In this particular instance, the purpose is to discover photographs that include essential features that fit the parameters of each enquiry. The questions can be interpreted in a variety of ways; hence, the best photographs will incorporate characteristics that are seen in a number of different pictures and will not necessarily have a strong connection to just one of the questions. This is due to the fact that the queries might have a range of different meanings. This is due to the fact that the queries have various interpretations, which explains why this phenomenon takes place. The retrieval of knowledge using a given question and the retrieval of information using a start with an empty space multiple query both present challenges that are fundamentally separate from one another. This is due to the reason that was stated before in this paragraph. Because the query photographs will not have the same low-level attributes in this scenario, the usefulness of constructing an averaged query will be diminished. Because the relevant photos do not essentially exhibit character traits that are closely related with a particular query, the vast majority of the extraction methods that are typically used are not suitable for use in this context. This is due to the fact that most retrieval methods are not suitable for use in this setting. For example, in order to solve this problem using methods of the bag-of-words kind, which could appear to be an obvious solution at first glance, the target image needs to have a strong connection to a number of the queries. This is required in order to proceed with the procedure. Submitting each query on its own and then determining the typical measure of correlation that exists between both the sets that are generated is an additional prevalent technique. This strategy is used rather frequently. If you do this, you will almost always end up with photographs that are very relevant to one of the questions, but you will almost never get pictures that are relevant to all of the questionnaires at the very same time. Because many more multiple query retrieval methodologies are being designed exclusively for the single complaint, they also have a tendency to attract images that are interconnected to only one or a few of the queries. This is because of the nature of the single-semantic-many-question problem.



1 2 3



4 5 6



7 8 9



10 11 12

Figure 1 The photographs that are located on the initial Pareto front are the ones that are returned when there are several requests made for the same set of photographs. The semantic information that may be retrieved from both of the query images has been combined into the photographs that are situated in the middle of the main page.

The insight that the middle of the Pareto front is quite essential when it comes to multiple query retrieval concerns is one of the most significant items that can be taken away from this body of work. This is one of the most important things that can be taken away from this body of work. The point upon that Pareto front and then corresponds to the precise midway of the front is known to as the median of something like the points on the front. This term is used to distinguish this point from the other points on the front. covers research on locating the centre of the Pareto front and the features that make such Pareto spots beneficial. [Coverage] also includes the features that make such Percentile spots beneficial. This project also includes some work on locating the center of the Pareto front, which is an important part of the analysis. It is possible to organize in a linear form a grouping of the points on the Pareto front that correspond to the three questions, and one can then compute the median as one would ordinarily do so. This is achievable thanks to the fact that the three questions can be grouped together. When there are more than two questions, rather of merely using the median itself, a multidimensional generalisation of the median, such as the mediod or the L1 median, can be used to find the front's center. This is because the median is a unidimensional statistic. This is due to the fact that the median is a statistic that only has two dimensions, which explains why this is the case. Figure 1 displays the photographs that comprise the initial Pareto front for a collection of images resulting from the execution of numerous queries. Both of these pictures depict different aspects of the same natural setting: a forest and a mountain. This is meant to act as an explanation in order to help illustrate the notion, and that is the goal of this. As the book is read, the illustrations are revealed one after the other in the order in which they are introduced at the beginning of the book, traveling in a clockwise direction from one page to the next. Even while there is a possibility that the images at the front's head and tail do not necessarily share any features with the other image under investigation, they are located in a rather close proximity to that image. As can be seen in Figure 1, the outcomes of both searches may be observed in the photographs that are located in the middle of the front (such as images 10, 11, and 12). These images feature important elements in their composition. Because they contain characteristics such as these, which are contained in the photographs, these pictures are very helpful for resolving the issue of several queries being used to retrieve the information. Our search technique was geared on locating photographs that fell into this particular category, and it was developed in order to locate these images. Even in situations in which the Pareto fronts do not have a convex shape, it is well known that the Pareto front technique can provide a large number of good solutions. One of the many instances in which this is the case is the one that we are discussing now. In this article, we present a new theory that, depending on the size of the database, either characterizes the asymptotic convexity of Pareto fronts or indicates that it does not exist. In other words, the theory may either prove or disprove the existence of asymptotic convexity.

This result was able to be derived because in topologically finite set theory, a link between The fronts and chains was constructed. This link allowed for the conclusion to be drawn, hence it was possible to reach this conclusion. A data point can only be considered to be on the Pareto front for a given depth if it is possible to create a maximal chain of length n. If this is not possible, then the data point cannot be considered to be on the Pareto front. A data point is not considered to be within the Pareto front of depth n if there is no possibility that it might lead to the construction of a chain of this kind. Because of this relationship, we are able to make use of the published studies that were done on the involves a great deal problem, which has a long history in probability and combinatory. This challenge involves finding the longest possible chain of consecutively increasing lengths. Finding the chain with the longest conceivable series of successively increasing lengths is the objective of this challenge.

The fact that the Pareto fronts are asymptotically convex when the dataset is taken into consideration is the most significant thing that can be learned from this inquiry. The fundamental conclusion that may be drawn from this is represented by theorem 1.

Consider several random variables that are completely unrelated to one another and are characterized by a continuous, separable, log-concave density function, which is represented by the notation f: [0, 1]d (0,). This theorem illustrates that our proposed solution will be of particular utility in cases in which the underlying density does not have a log-concave form. In other words, these are instances in which the log-concave shape would not be appropriate. The majority of the time, the underlying density does not even have a quasi-concave shape, as shown by the numerical data that we present in Figure (2b), which may be found below. Taking a look at the graph should make this very clear. This helps to explain why the performance of our proposed Pareto front technique experienced an improvement when it was applied. In addition to this, we highlight the fact that our PFM approach has the potential to be exploited for the automatic photo annotation of big databases by pointing out that this is something that can be done. Since images in the middle of the first few Pareto fronts are relevant to all searches, one could issue various question combinations with known class labels or other metadata, and then automatically annotate the images in the middle of the first few Pareto fronts with the metadata from the queries. This would be possible because images in the middle of the first few Pareto fronts are relevant to all searches. The purpose of this project is to automatically assign keywords, classifications, or captioning to images that are stored in a database that has either no annotations or annotations that are of a poor quality.

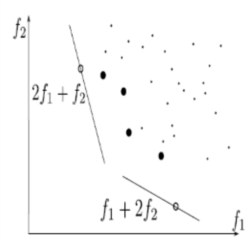

(a)

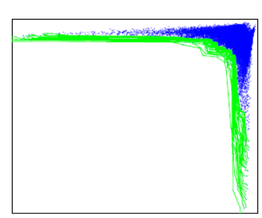

(b)

Fig 2. (a)Depiction of nonconvexities in the first Pareto front.(b)Depiction of nonconvexities in the Pareto fronts in the real-world Mediamill dataset.

II. PROPOSED METHOD

This article demonstrates a one-of-a-kind method for retrieving a large number of photos using a variety of different queries. This technique ranks items using both the efficient manifold ranking and the Pareto front method (PFM). The purpose of the system is to extract the best photographs from a database while at the same time conducting as few searches as is practically practicable for a person (EMR). Our PFM technique starts by generating a unique query for each example in the database. After that, it gives a score to each sample based on the extent to which it resembles or detracts from the query that was provided. It is feasible to compute the dissimilarities of images by making use of any of the approaches that are presented in the computer vision literature for the aim of computing image representations. These methods are all geared toward the same end goal. The SIFT and HoG methodologies are two good examples of such approaches. Because it is computationally difficult to compute the dissimilarities for each sample-query combined effect in large amounts of data, we use a quick ranking algorithm known as Efficient Manifold Ranking (EMR) to calculating the ranking without putting into account all sample-query pairs. This is because it is computationally difficult to compute the inconsistencies for each sample-query combination in large datasets. We are able to cut down on the amount of data that processes the data as a result of this. When working with large databases, it is possible to determine the inconsistencies for each sample-query pair by using the inconsistencies between the sample and the query alone. This is done in huge databases. EMR is able to uncover the fundamental geometric of the building in a way that is more efficient in terms of both time and labor. Non-dominated sorting is the term used to describe the process of arranging points in Pareto fronts [6].

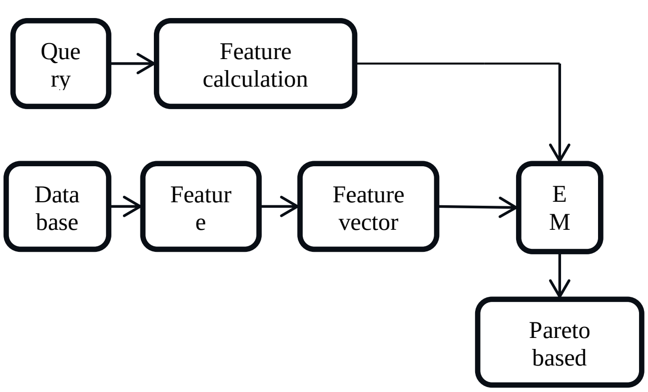

Fig. 3. Block diagram for the proposed method.

III WORK CONNECTED TO THIS PROBLEM

A.HISTOGRAM OF ORIENTED GRADIENT

The histogram of oriented gradient is a feature descriptor that is used in computer vision and image processing to facilitate object detection. This recognition is achieved by the use of this feature descriptor. By tallying the number of times each gradient orientation appears in a particular section of an image, this method calculates the total number of gradient orientations that can be found in that area.

1.Gradient calculation

The computation of the values of the gradient is the initial step of the calculation that needs to be completed. This phase of the calculation must be completed. In the vast majority of instances, the 1-D centred,point discrete derivative mask is applied in either the horizontal or the vertical direction, or both. In some instances, the mask is applied in both directions. It is also possible to use it in the opposite direction on occasion. This can be accomplished going either forward or backward. The processing of the image's color or intensity data using the particular filter kernels that are stated below is required in order to have this strategy result in a successful conclusion:

$[-1, 0, 1]$ and $[-1, 0, 1]^T$

2. A categorization of the many orientations

The production of cell histograms is the second stage involved in the process of carrying out the calculation. Each pixel that is included within the cell casts a vote for a certain orientation-based histogram channel, and the votes are weighted accordingly. The values that are revealed by the computation of the gradient are what determine the weight that should be assigned to each vote. Depending on the geometry of the cells, which can be either rectangular or radial, it is feasible for the histogram channels to be evenly distributed throughout a range of 0 to 180 degrees or 0 to 360 degrees. This is because the cells can take either of these two shapes.

The gradient can be described as "unsigned" or "signed," depending on your preference. In the human detection tests that Dalal and Triggs carried out, they found that the best results came from utilizing unsigned gradients in conjunction with 9 histogram channels. This combination produced the best overall results.

3. Descriptor blocks

In order for the gradient strengths to be able to account for fluctuations in the illumination and contrast, they need to be normalized on a local basis. In order to achieve this goal, the individual cells will need to be organized into larger blocks, which will then need to be connected to one another geographically. As a result, the HOG descriptor refers to the vector that contains the components of the normalized cell histograms for each of the block sections. This vector may be found in the previous sentence. The fact that these blocks frequently overlap one another demonstrates that each individual cell contributes significantly to the full description. In the vast majority of situations, this is how things play out.

There are two basic block morphologies, and they are referred to as circular C-HOG blocks and rectangular R-HOG blocks, respectively. C-HOG stands for circular head-on-grid, and R-HOG is for rectangular head-on-grid. Every R-HOG block is defined by three parameters: the number of cells that make up the block, the number of pixels that make up each cell, and the number of channels that make up the histogram for each cell. Each of these numbers can be found in the block's histogram. Blocks that are members of the R-HOG family are frequently placed in the shape of square grids.

Fig 4(a). Initial image

This same standardized representation of the primary constituents A wide variety of methods can be utilized to successfully complete the block normalizing process. Let us make the assumption that is the non-normalized vertex that contains all of the histograms in the specified block, that k is its k-norm for k equal to 1, and that e is indeed a very small constant that represents this same exact value of the histogram. If we do this, we can determine the exact value of the histogram (which, ideally, is insignificant). The normalization factor might therefore be any of the following scenarios:L2-norm:

$$f = \upsilon / \sqrt{|| \upsilon ||_2^2 + e^2}$$

L1-norm:

$$f = \upsilon / || \upsilon ||_1 + e)$$

L1-sqrt:

$$f = \sqrt{\upsilon} / (|| \upsilon ||_1 + e)$$

Fig 4(b). X derivative of initial image

Fig 4(c). Y derivative of initial image

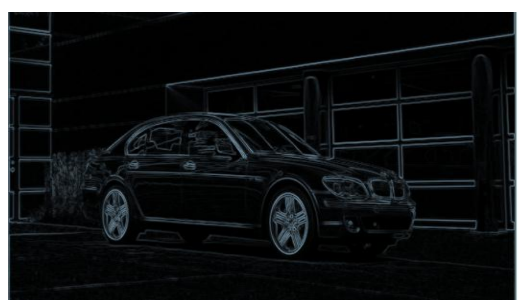

Fig 4(d). Magnitude of Gradient

B. PARETO FRONT METHOD

[15] Computer science, economics, and the social sciences are just a few of the fields in which the concept of Pareto-optimality has been put into practice. We present to her for consideration an overview of Pareto-optimality as well as an

explanation of the concept of a Pareto front, both of which are shown below in their respective forms. In the context of an instance that has never been seen before of a discrete multi- have a limited set S of viable solutions and T criteria f1,..., fT: S R for evaluating the available solutions in the issue space for an objective optimization problem. One of the potential objectives is to identify whether or not x is bigger than S while simultaneously lessening the weight that each of the factors carries in the overall evaluation. It is not possible to achieve this objective in the vast majority of scenarios. There are many various approaches to multi-objective optimization, and the first step in each of these approaches is to integrate all T criteria into a single criterion. In other words, this is the beginning point. This method is referred to as linear scalarization the vast majority of the time, and it is executed by making use of linear combination. This is the case since linear combination is the most straightforward way to carry it out. The linear combination has the potential to produce a wide range of unique minimizers; however, the realization of this potential is dependent on the weights that are employed in the process. It is important to carry out a grid search through all of the available weights in order to locate a set of solutions that are credible because there is no previous information regarding the relative value of each criterion.

A methodology that is more principled and dependable is the one that conforms to the Pareto principle in order to determine which solutions are the best potential ones. If there isn't another option that performs better than this one overall, then we refer to this one as the Pareto-optimal solution. If the comparison reveals that the value of fi (x) is greater than the value of fi (y) for all I, and if the comparison reveals that the value of f j (x) is more than the value of f j (y) for at least one j, then it is evident that x is more important than y. When assessing whether or not a piece x S is in the Pareto-optimal location, one must examine whether or not it is strictly dominated by another piece. If it is, then the piece is not in the Pareto-optimal location. The group of viable options that, from a Pareto analysis point of view, are in the best possible position is what is meant when people talk about the "first Pareto front." It takes into consideration all of the answers that may be acquired via the use of linear scalarization as well as the aspects that linear scalarization does not take into consideration. The letter F1 indicates the beginning of the chart that represents the Pareto principle. After removing the first Pareto front from S and determining the Pareto front of the data that was still available to you, you would have been able to obtain the second Pareto front, which is represented by the symbol F2. After you computed the Pareto front for the data that was not used, this would have been the case. The ith Pareto front can be described in a number of different ways, one of which is as follows:

= The point in the Pareto distribution for set S at which the slope of the distribution begins to rise.

When x has a value that is less than Fk, we say that it has a Pareto depth of k. If Fk is greater than x's value, then it does not have a Pareto depth. If option I is chosen first, then the Pareto front F will have a wider coverage area than the Pareto front Fj will. Figure 2(a) is an easy-to-understand representation of the value that may be contributed to the ranking process by making use of Pareto front techniques. This value may be in the form of a higher probability of a certain item being ranked higher. Because there are two criteria applicable to this particular scenario, the number of criteria is denoted by the letter T. The Pareto points, [f1(x), f2(x)], with x ranging from 0 to S in the range of values are depicted in Figure 2. (a). In this figure, the huge points represent the Pareto optimal solution; yet, using linear scalarization, only the hollow points may be recovered as the top ranking items. This is because linear scalarization only takes into account the distance between points. This is due to the fact that the larger points are packed more tightly together than the smaller points. Figure 2 is an illustration of the well-known fact that linear scalarization can only produce Pareto points on the boundary of the convex hull of the Pareto front. This is the only location where Pareto points can be produced. (a). This is a fact that is acknowledged by the majority of people. Even for Pareto fronts that have a greater depth to them, this observation is true. Figure 2(b), which depicts the Pareto fronts for the multiple-query retrieval problem, uses real data obtained from the Mediamill dataset to illustrate the problem. These data are used to show the multiple-query retrieval problem. This particular illustration demonstrates the nature of the issue in question. Take note of the extreme absence of convexity that characterizes the limits of the genuine Pareto fronts shown in Figure 2; this is something that you should be aware of. (b). This is a highly significant finding, which has direct bearing on the fact that each question correlates to a distinct visual meaning. This discovery is directly tied to the fact that. This insight can be traced back to the observation that each inquiry corresponds to a distinct visual meaning. Because of this, there are no images that are excellent matches for both of the searches at the same time. This is a direct consequence of this.

The letter C represents the effective ranking of the manifold (EMR)

Let us make the assumption that the collection of points that is denoted by X = X1,..., Xn Rm represents a finite collection of points and that the metric that is denoted by d: X R, such as the Euclidean distance, represents a distance measure that is applicable to X. Let us also make the assumption that the collection of points that is denoted by Rm represents a finite collection of points. Let us also assume that the collection of points denoted by X is a finite one. This would mean that the set of points represented by X is limited in size. You are going to refer to the vector that you create as y, and you are going to give it the following parameters: [y1,..., yn] The value of yi should be 1 if the statement Xi is in the form of a question; however, it should be 0 in all other circumstances. The ranking function is implemented by assigning a ranking score ri to each point Xi in the data collection; the notation r:X R will be used to describe this function. This makes it possible for the ranking mechanism to operate. With the help of this function, the points are arranged in a hierarchy that goes from least valuable to most valuable, with the least valuable points coming first. The inquiry is given the highest possible rank, which is 1, and each of the other samples is given a rank that is proportionate to their distance from the inquiry along the manifold that underlies the data. The distance between the two is measured along the data's underlying manifold. You should first sort the components into paired groups before establishing a network with X.sdistances between all of the samples ordered in descending order. This will ensure that the network is constructed correctly. After that, as you proceed with the construction of a linked graph G until it is complete, you should add edges between points according to this order while doing so. This graph shows the value wij, which signifies the edge weight that is related with the connection that already existing between Xi and X j. You can see it presented here. If there is an edge connecting Xi and X j, define the weight as wij = exp[d2(Xi, X j)/22. If there isn't an edge connecting the two nodes, let wi j = 0 and define W as (wi j)i j Rnn. Define the weight as wij = exp[d2(Xi, X j)/22 if there is an edge linking Xi and X j. If there is such an edge, If Xi and X j are linked together by an edge, the weight can be calculated as follows: wij = exp[d2(Xi, X j)] (Xi, X j) The cost function that is associated with ranking vector r can be defined as in terms of the manifold ranking approach.

Where D is a diagonal matrix and >0 is a parameter for the regularization that must be greater than zero. The smoothness term, which appears first in the cost function, is in charge of ensuring that points that are relatively close to one another have comparable ranking scores. This is because the smoothness term comes first in the cost function. The second term is referred to as a regularisation term, and its purpose is to ensure that the rank of the query is as close to 1 as is humanly possible, while also ensuring that the ranks of all other samples are as close to 0 as is humanly possible. This is accomplished by ensuring that the regularisation term ensures that the rank of the query is as close to 1 as is humanly possible. To achieve this goal, it is necessary to make certain that the ranks of all of the other samples are as indistinguishable from zero as is humanly possible. The ranking function designated by the letter r is the function that, in comparison to all of the other possible ranking functions, obtains the lowest value for the parameter O(r).

The current optimization problem has two potential resolutions: either it may be addressed directly, or it can be solved indirectly through an iterative procedure. Both of these strategies will be broken down in the following paragraphs. To produce an accurate response, use the closed-form expression r = (In S) 1 y, where = 1/1+, In is an identity matrix that is n by n, and S = D1/2WD1/2. This will allow you to acquire the desired result. This will result in the identification of the appropriate response. This particular form of operation is referred to as a "direct approach," which is an industry phrase. When applied to datasets of a significant size, the iterative approach reveals itself to be the most efficient way. The ranking function r is calculated by repeatedly using the iteration scheme r (t + 1) = Sr(t) + (1)y until the function reaches a point of convergence. When the function reaches this point, the ranking function is deemed to have arrived at its ultimate value. The iterative method calls for a memory that is n by n and may converge to a local minimum, whereas the direct method calls for the inversion of a matrix that is n by n. The direct approach is, nevertheless, the choice that results in more productivity. In addition, the degree of complexity that is involved in the process of creating the graph G is O. (n2 log n) (n2 log n). When one employs a kNN graph, as is sometimes the case, the complexity of the graph G is decreased to O. (kn2) (kn2). For the aim of finding answers to problems that affect a large number of people, neither of these scenarios is an alternative that can be considered acceptable. A weight matrix Z'Rd'n that assesses the possible associations that could exist between the data items in X and the anchors in U. This matrix evaluates the possible relationships between the two sets of data. In the sake of avoiding confusion and keeping things as simple as possible, we are going to refer to the ith column of Z as zi. The affinity matrix W is then constructed after this stage so that it is ZT Z, and the final ranking function r can then be directly computed by applying the formula = H). This step concludes the process.

In the case where H = ZD1/2 and D is a diagonal matrix with =, this method requires inverting only a d d matrix, whereas the regular manifold ranking method requires inverting a n n matrix. This is owing to the fact that diagonal matrices are utilized in the typical manifold ranking method. When both d and n are very large, as they almost always are in huge databases, the amount of computer power required to perform manifold ranking is drastically reduced. The use of the EMR method to compute the ranking function is represented by the notation O (dn+ d3), which stands for the complexity of the task. In addition to this, EMR does not require the storage of an n-by-n matrix in order to function properly.

IV. RESULTS AND DISCUSSION

In order to determine the gradient in the vertical direction for the vertical gradient and the horizontal direction for the horizontal gradient, the filtering strategy that will be used will involve applying the 1D centred point discrete derivative. This will be done in order to determine the gradient. In the process of computing the features, a histogram of the gradient orientation is employed, along with quantized levels for hue, saturation, and value. This is accomplished by dissecting the character's plans and analyzing each one separately before putting them back together again. Using a method known as color correlogram, it is possible to extract the spatial information that is held within the pixels of an image. This can be done in a number of different ways. The explanation of what is meant by the term "Orientation," in its most basic form. One-dimensionality can be attributed to smaller image portions on a more local scale depending on the lines or edges that are present in those particular sections of the image. This is something that can be accomplished.

V. CONCLUSION

Our group has come up with and presented a brand-spanking-new strategy for retrieving content-based images using many queries at once. The method's goal is to locate images that are a match for each and every one of the questions that have been posed, and the questions themselves cover a wide variety of topics pertaining to the semantics of images. Our approach is able to complete this task with a reasonable amount of ease, in contrast to existing multiple-query retrieval strategies and linear scalarization methods which may have difficulty recovering particular samples. We have offered theoretical arguments that demonstrate why the Pareto technique is preferable to linear combinations of ranking outcomes, and these arguments are presented here. These findings are derived from the asymptotic fact that Pareto fronts are not convex in their shape. Based on these findings, it appears that the Pareto method generates more trustworthy conclusions than other methodologies.

REFERENCES

[1] Li, X., Epitropakis, M. G., Deb, K., & Engelbrecht, A. (2016). Seeking multiple solutions: an updated survey on niching methods and their applications. IEEE Transactions on Evolutionary Computation, 21(4), 518-538.

[2] Garcia, D., Lugo, A. E., Hemberg, E., & O'Reilly, U. M. (2017, July). Investigating coevolutionary archive based genetic algorithms on cyber defense networks. In Proceedings of the Genetic and Evolutionary Computation Conference Companion (pp. 1455-1462).

[3] Abdikenov, B., Iklassov, Z., Sharipov, A., Hussain, S., & Jamwal, P. K. (2019). Analytics of heterogeneous breast cancer data using neuroevolution. IEEE Access, 7, 18050-18060.

[4] Hesselbach, X., Fabregat, R., Baran, B., Donoso, Y., Solano, F., & Huerta, M. (2005, October). Hashing based traffic partitioning in a multicast-multipath MPLS network model. In Proceedings of the 3rd international IFIP/ACM Latin American conference on Networking (pp. 65-71).

[5] Bharti, V., Biswas, B., & Shukla, K. K. (2021). A novel multiobjective gdwcn-pso algorithm and its application to medical data security. ACM Transactions on Internet Technology (TOIT), 21(2), 1-28.

[6] Vipsita, S., & Rath, S. K. (2012). Protein superfamily classification using adaptive evolutionary radial basis function network. International Journal of Computational Intelligence and Applications, 11(04), 1250026.

[7] Chvatal, V. (1979). A greedy heuristic for the set-covering problem. Mathematics of operations research, 4(3), 233-235.

[8] Fabregat, R., Donoso, Y., Baran, B., Solano, F., & Marzo, J. L. (2005, October). Multi-objective optimization scheme for multicast flows: a survey, a model and a MOEA solution. In Proceedings of the 3rd international IFIP/ACM Latin American conference on Networking (pp. 73-86).

[9] Gallego, A. J., Calvo-Zaragoza, J., Valero-Mas, J. J., & Rico-Juan, J. R. (2018). Clustering-based k-nearest neighbor classification for large-scale data with neural codes representation. Pattern Recognition, 74, 531-543.

[10] Freitas, D., Lopes, L. G., & Morgado-Dias, F. (2020). Particle swarm optimisation: a historical review up to the current developments. Entropy, 22(3), 362.

[11] Gallego, A.J., Calvo-Zaragoza, J., Valero-Mas, J.J. and Rico-Juan, J.R., 2018. Clustering-based k-nearest neighbor classification for large-scale data with neural codes representation. Pattern Recognition, 74, pp.531-543.

[12] Vipsita, Swati, and Santanu Ku Rath. "Protein superfamily classification using adaptive evolutionary radial basis function network." International Journal of Computational Intelligence and Applications 11, no. 04 (2012): 1250026.